ISCI, Volume *13*

Supplemental Information

Conjugated Polymers with Oligoethylene Glycol Side Chains for Improved Photocatalytic Hydrogen Evolution

Zhicheng Hu, Zhenfeng Wang, Xi Zhang, Haoran Tang, Xiaocheng Liu, Fei Huang, and Yong Cao

Supplemental Information

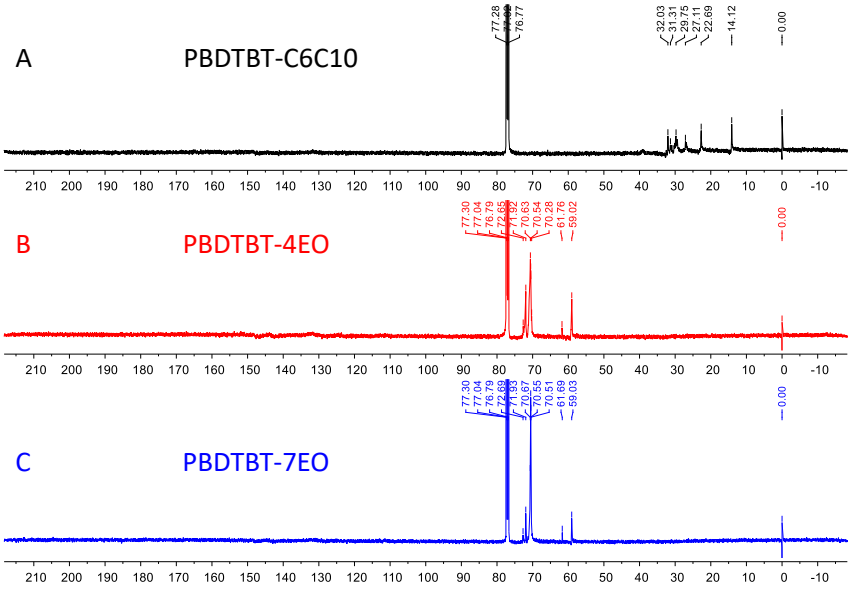

Figure S1. ^{13}C NMR spectra of PBDTBT-C6C10(A), PBDTBT-4EO(B), and PBDTBT-7EO(C) in $CDCl_3$, related to Figure 1. The aromatic carbon signals of these three polymers are difficult to detect due to strong aggregation of these polymer in solvents. The carbon signals of their side chains can be observed, which exhibit chemical shifts of alkyl side chains for PBDTBT-C6C10 and oligoethylene glycol for PBDTBT-4EO and PBDTBT-7EO, respectively.

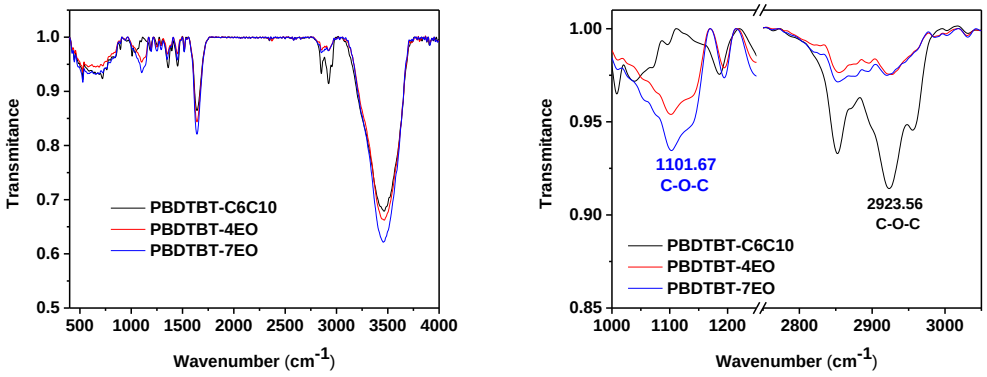

Figure S2. FT-IR spectra of PBDTBT-C6C10, PBDTBT-4EO and PBDTBT-7EO powders, related to Figure 1.

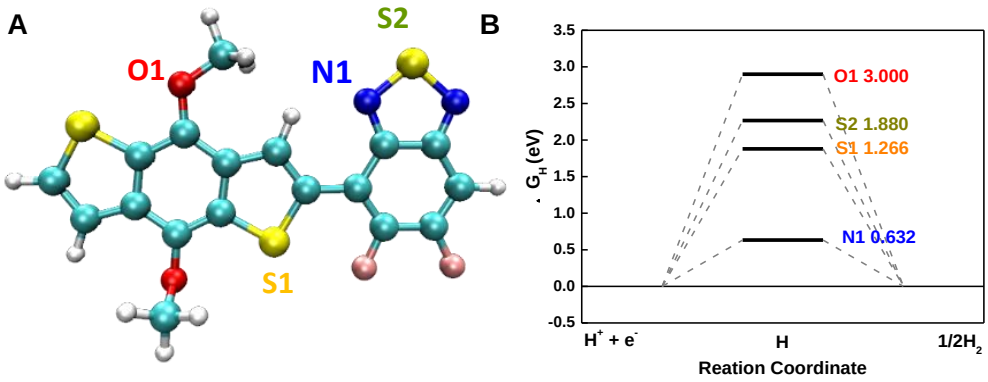

Figure S3. The calculated hydrogen binding free energy (ΔG_H) of heteroatom in backbones of PBDTBT, related to Figure 1. The calculations were performed at the level of B3LYP-D3(BJ)/def2-TZVP.

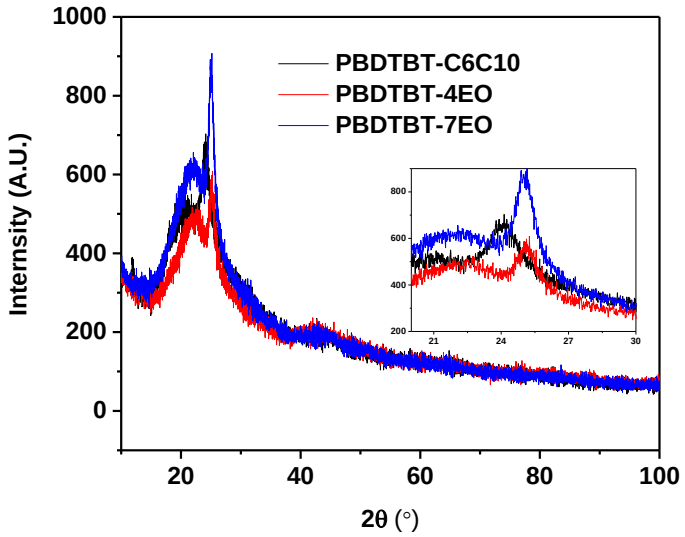

Figure S4. XRD results of conjugated polymers, related to Figure 1. The clear peaks of PBDTBT-C6C10, PBDTBT-4EO and PBDTBT-7EO are located at 24.06°(2θ), 25.11°(2θ)and 24.99°(2θ), corresponding to π–π distances of 3.700 Å, 3.565 Å and 3.548 Å.

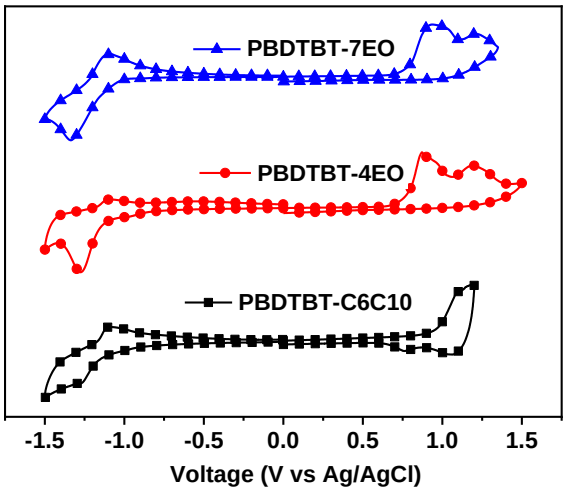

Figure S5. The cyclic voltammetry curves of these polymers, related to Figure 1.

Figure S6. Water contact angles of (A) PBDTBT-C6C10, (B)PBDTBT-4EO, and (C) PBDTBT-7EO films, related to Figure 1.

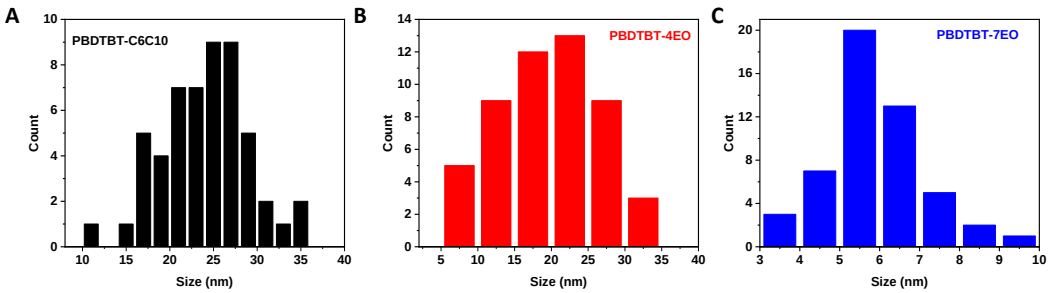

Figure S7. Size distribution of conjugated polymer nanoparticles in water calculated from TEM via image analysis software over 50 nanoparticles, related to Figure 2. PBDTBT-C6C10: 24.1±5.1 nm; PBDTBT-4EO: 19.7±6.5 nm; PBDTBT-7EO: 5.9±1.1 nm.

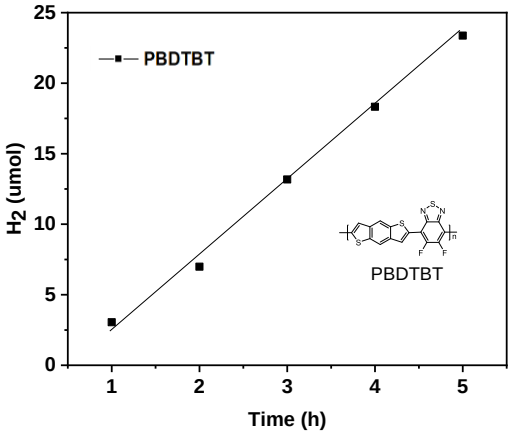

Figure S8. Hydrogen evolution of PBDTBT, related to Figure 3.

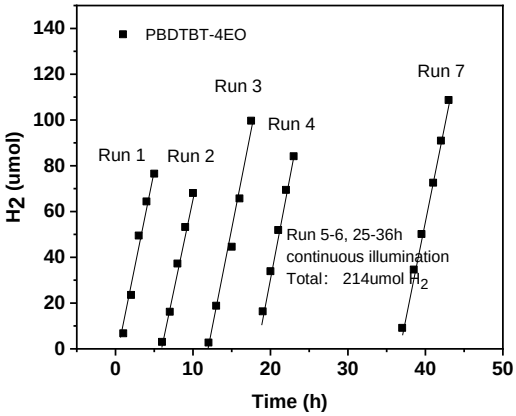

Figure S9. Hydrogen evolution of PBDTBT-4EO with over long-time illumination, related to Figure 3. Average HERs of 18.03 μmolh^{-1} for Run 1, 16.7 μmolh^{-1} for Run 2, 17.07 μmolh^{-1} for Run 3, 17.08 μmolh^{-1} for Run 4, 16.4 μmolh^{-1} for Run 5-6, 16.4 μmolh^{-1} for Run 7.

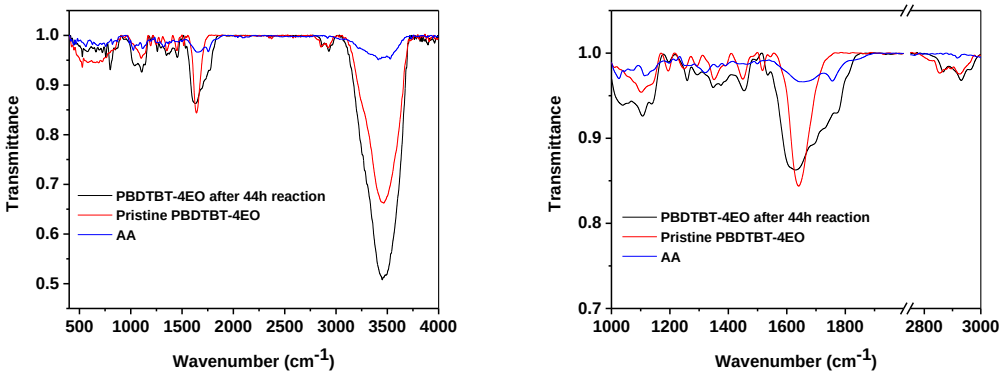

Figure S10. FT-IR spectra of PBDTBT-4EO before and after 44h reaction, related to Figure

3. The FT-IR spectrum of PBDTBT-4EO after reaction is a mixture of the spectra from AA and PBDTBT-4EO, indicating that chemical structure of PBDTBT-4EO 44h reaction is stable.

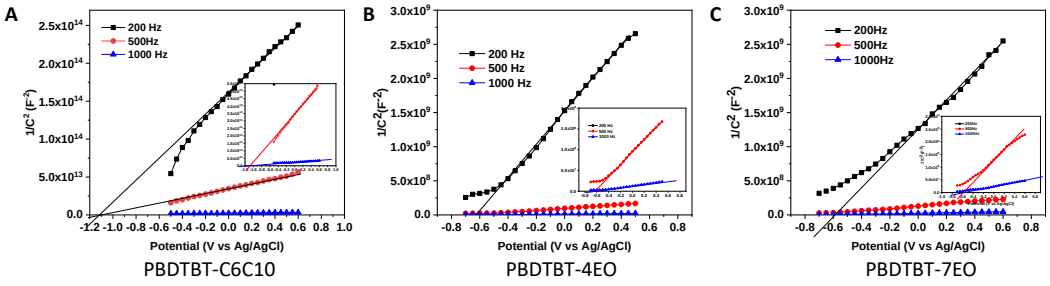

Figure S11. Mott–Schottky plots of PBDTBT-C6C10, PDBDTBT-4EO, and PBDTBT-7EO in 200Hz, 500Hz and 1000Hz, related to Figure 4.

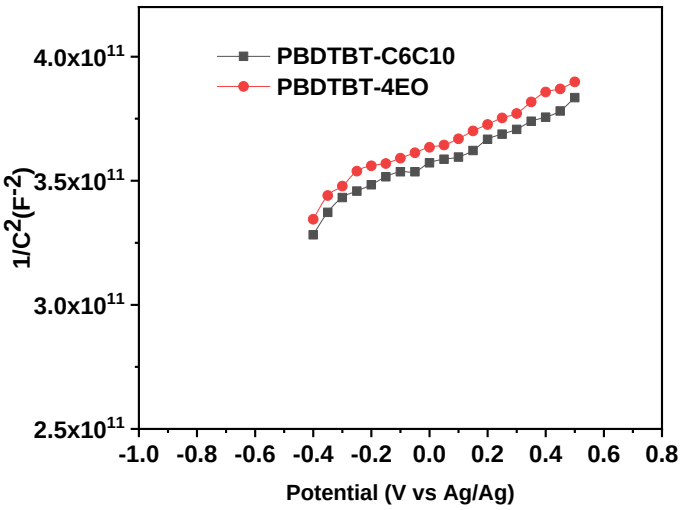

Figure S12. Mott–Schottky plots of PBDTBT-C6C10, and PDBDTBT-4EO in in anhydrous acetonitrile, related to Figure 4.

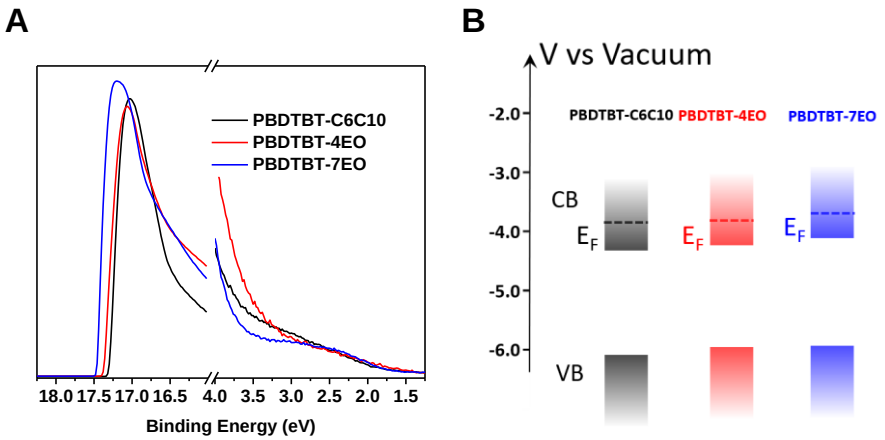

Figure S13. (A) UPS spectra and (B) energy band positions of PBDTBT-C6C10, PBDTBT-4EO, and PBDTBT-7EO, related to Figure 4.

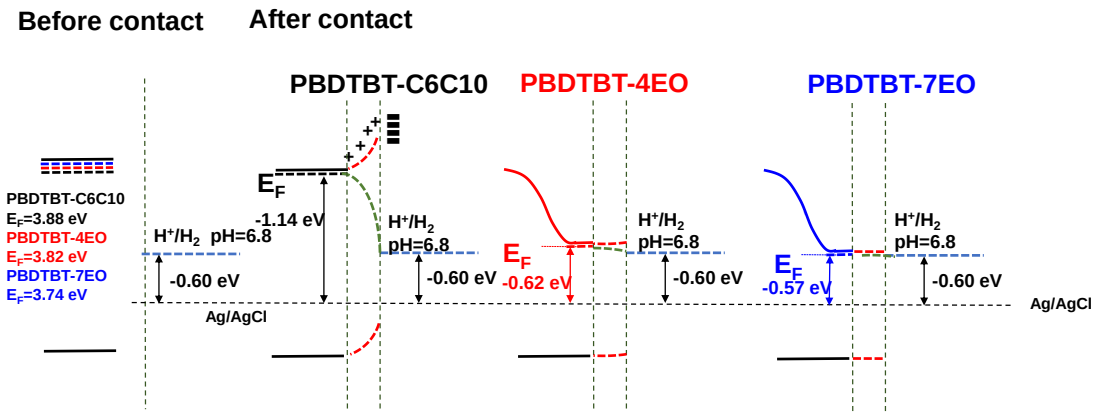

Figure S14. The fermi levels of PBDTBT-C6C10, PBDTBT-4EO and PBDTBT-7EO in the state of before and after contacting with water, related to Figure 4. The fermi levels before contact were determined by UPS, while the fermi levels after contact were determined approximately by E_{FB} referred to the redox potential of electrolyte.

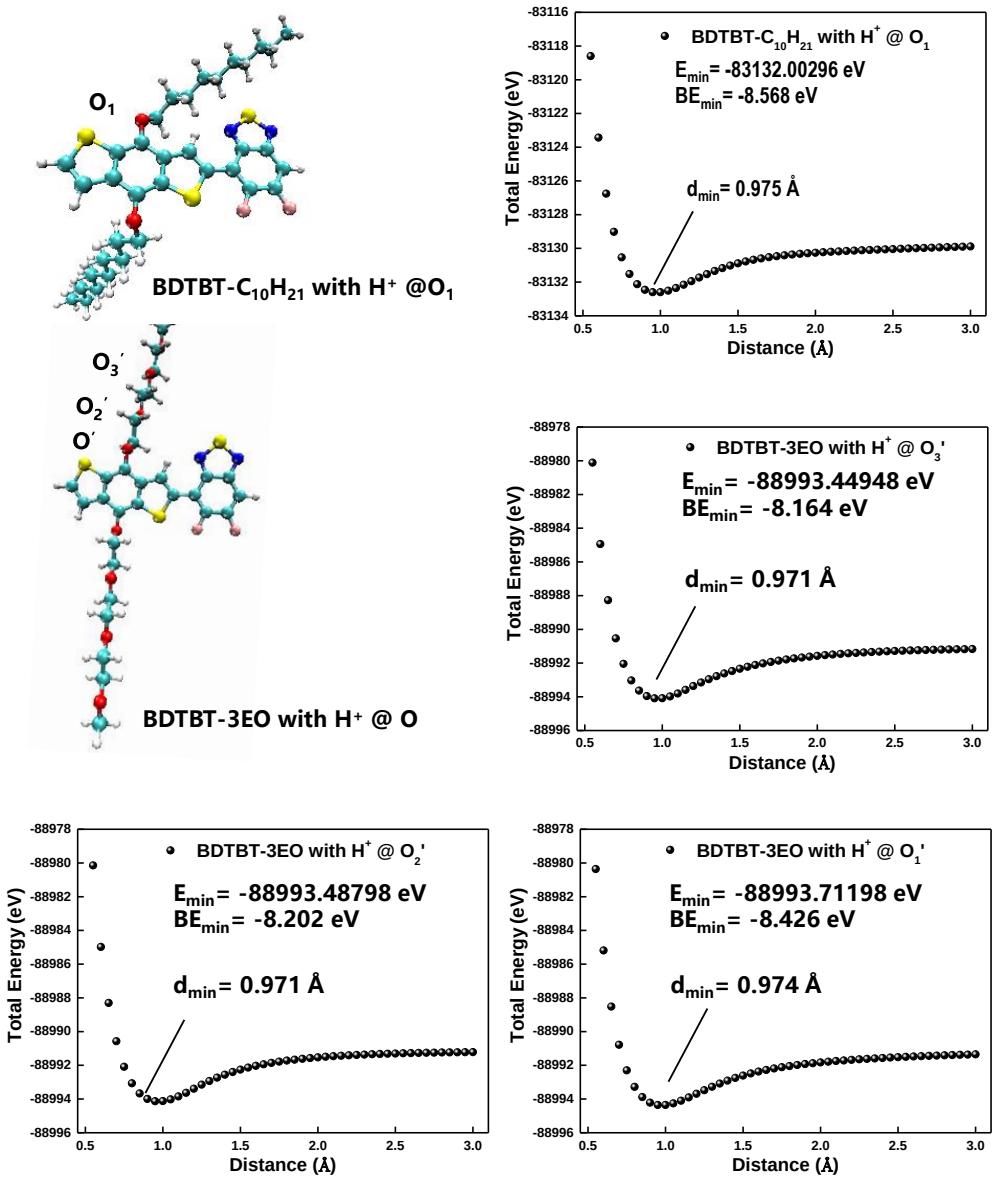

Figure S15. The total energy vs distance plots of BDTBT-$C_{10}H_{21}$ and BDTBT-3EO with one H^+ absorbed in oxygen, related to Figure 5. The minimum contact distances are around 1 Å, and the minimum binding energy can be obtained.

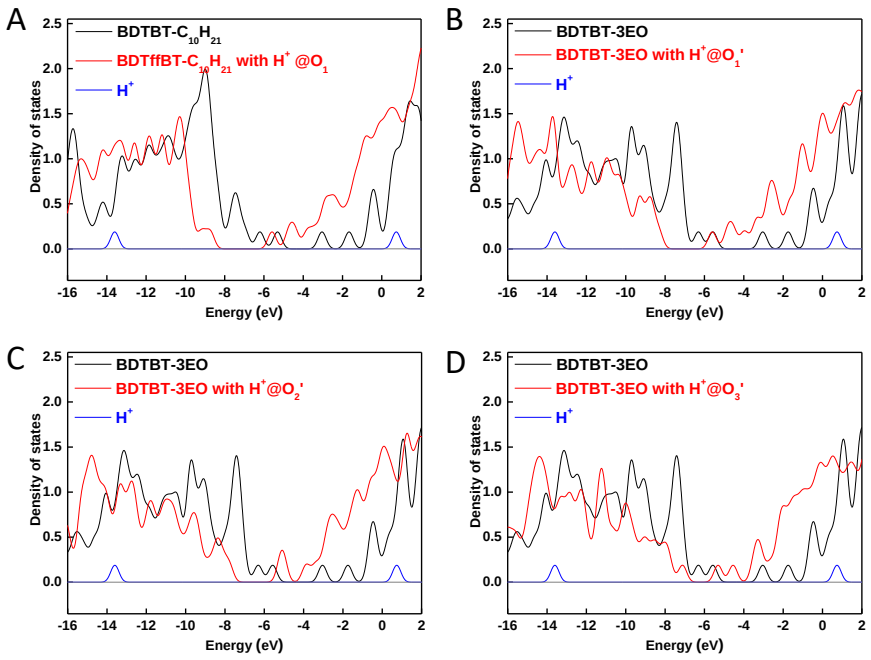

Figure S16. DOS state of BDTBT-$C_{10}H_{21}$ (A) and BDTBT-3EO (B-D) with H^+ absorbed oxygen sites (the case of one hydrogen atom), related to Figure 5.

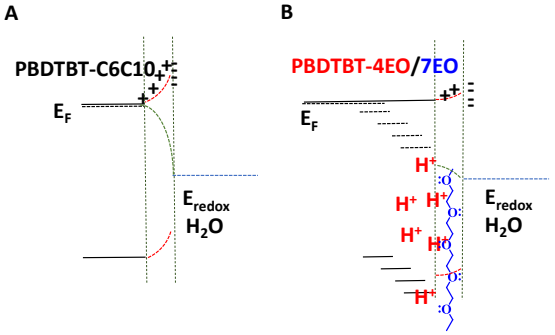

Figure S17. Scheme diagram of energy level changing of (A) PBDTBT-C6C10 and (B) PBDTBT-4EO/7EO in contact with water, related to Figure 5.

Table S1. Performance summary of linear conjugated polymeric photocatalysts, related to Figure 3.

Catalysts	HER (mmol $h^{-1}g^{-1}$)	AQY (wavelength)	Reaction Conditions	Abs. edge	Reference
PPP-11-Ru	0.3		TEA	450	Shibata et al., 1990
PBpy-Py$(bpy)_2$	2.55		H_2O /TEA	420	Maruyama et al., 1997
B-BT-1,4	2.32	4.01% (420 nm)	H_2O /TEOA	517 nm	Yang et al., 2016
Planarized Conjugated Polymer	5.8	2.3 % (420 nm)	H_2O/ CH_3OH /TEA	460 nm	Sprick et al., 2016
PPDI-bpy	0.355	0.02% (525 nm)	H_2O/DEA	600 nm	Li et al., 2016
PT/PVA-Pt		0.06%	MV^{2+}/EDTA	680 nm	Lu et al., 2017
PTh	2.8		AA/H_2O	650 nm	Zong et al., 2017
PFBT Pdots	8.3	0.5% (445 nm)	AA/H_2O	520 nm	Wang et al., 2016
PFODTBT dots (0.1% Pd)	Initial: 50.0 Average: 15.5 (4 h)	0.6% (550 nm)	AA/H_2O	650 nm	Pati et al., 2017
Conjugated copolymer:p8-i	0.86	0.56 % (420nm)	H_2O/CH_3OH /TEA	400 nm	Woods et al., 2017
PFTFQ-PtPy15	10.2 (4 h)	0.40% (515 nm)		610 nm	Tseng et al., 2018
PBDTBT-7EO (3.0 wt% Pt)	15.9	0.30% (600 nm)	AA/H_2O	720 nm	This work

Table S2. Performance summary of part polymeric photocatalysts, related to Figure 3.

Catalysts	HER ($mmolh^{-1}g^{-1}$)	AQY (wavelength)	Reaction Conditions	Abs. edge	Reference
g-C_3N_4 (3.0 wt% Pt)	0.1	0.1 %	H_2O/TEOA	450 nm	Wang et al., 2009
Triazine-based Carbon Nitrides (2.3 wt% Pt)	4.9	3.4%	H_2O/TEOA		Schwinghammer et al., 2013
g-C_3N_4 (3.0 wt% Pt)	15	50.7% (405 nm)	H_2O/TEOA		Lin et al., 2016
g-C_3N_4 (3.0 wt% Pt)	20	26.5%(400 nm)	H_2O/TEOA	450	Martin et al., 2014
g-C_3N_4	23.06	31.07% (420 nm)	H_2O/TEOA		Yu et al., 2018
Conjugated poly(azomethine) (3.0 wt% Pt)	0.07		H_2O/TEOA	510 nm	Schwab et al., 2010
Conjugated copolymer	0.18	4.2%	H_2O/TEOA	650 nm	Sprick et al., 2015
hydrazone-based COF (Pt-modified)	1.9	2.2 % (400 nm)	H_2O/TEOA		Stegbauer et al., 2014
azine hydrazone-based COF (0.68 wt% Pt)	1.5	0.45% (450 nm)	H_2O/TEOA	550 nm	Vyas et al., 2015
Microporous organic nanorods (TiO_2-Pt)	1.25	4.5%	H_2O/TEOA	540 nm	Park et al., 2014
Phenyl-triazine oligomers (2.2 wt% Pt)	0.12	5.5% (400 nm)	H_2O/TEOA		Schwinghammer et al., 2015
Conjugated Polybenzothiadiazoles (3.0 wt% Pt)	2.9	4.0% (420 nm)	H_2O/TEOA	550 nm	Yang et al., 2016
PFBT/C_3N_4 (1% Pt)	0.7	10.1% (500 nm)	H_2O/TEOA	560 nm	Chen et al., 2017
Porous Conjugated Polymers (2.0 wt% Pt)	0.17	1.8% (350 nm)	H_2O/CH_3OH/TEA	620 nm	Li et al., 2016

Transparent Methods

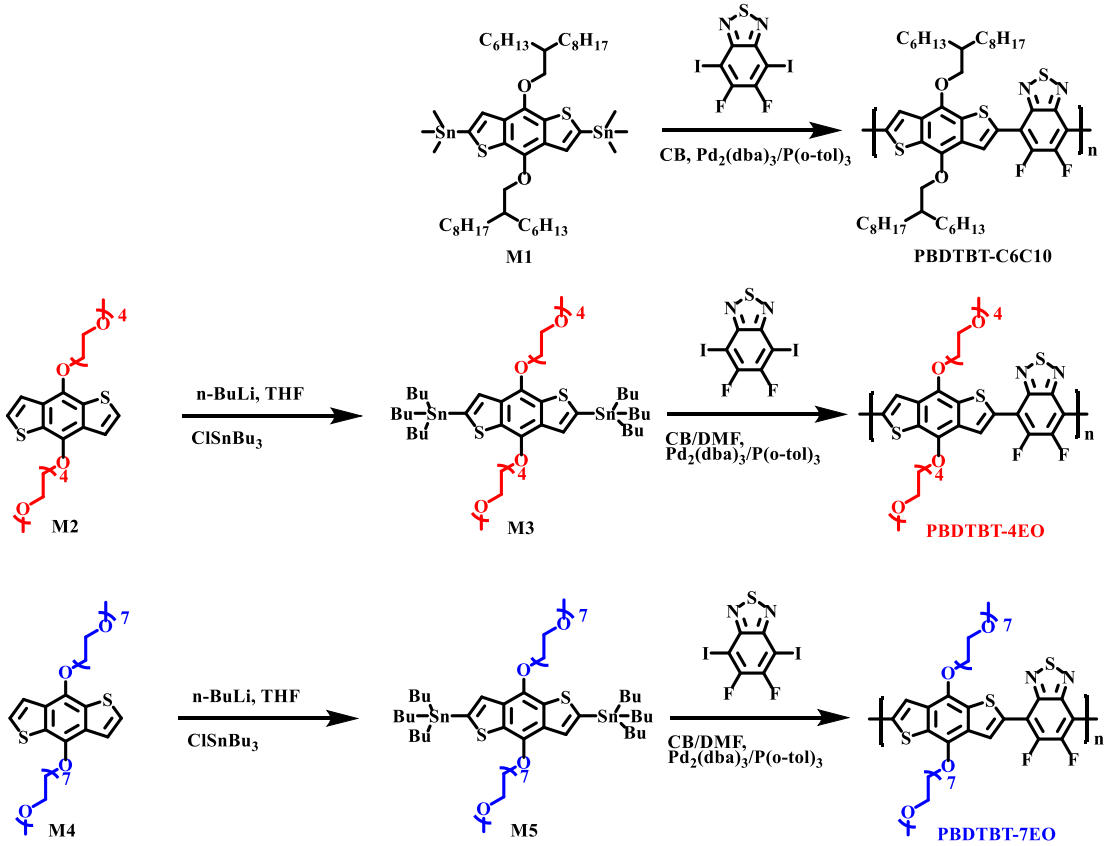

Scheme S1 Synthetic procedures of conjugated polymers, related to Figure 1.

Materials: M1 was purchased from Suna Tech Inc., and used after recrystallization from ethanol. 5,6-difluoro-4,7-diiodobenzo[c][1,2,5]thiadiazole was synthesized according to the published reference (Wang et al., 2013).

PBDTBT-C6C10: PBDTBT-C6C10 was synthesized from M1 and M2 using Stille polymerization in chlorobenzene (CB) in the existence of $Pd_2(dba)_3$ and tri(o-tolyl)phosphine ($P(o\text{-}tol)_3$). M1 (99.8 mg, 0.1 mmol) and 5,6-difluoro-4,7-diiodobenzo[c][1,2,5]thiadiazole (42.4 mg, 0.1 mmol) were placed in a round-bottomed flask, then CB (1.0 mL) was added. The mixture was then degassed for three times to remove the oxygen. Then $Pd_2(dba)_3$ (1.0 mg) and $P(o\text{-}tol)_3$ (2.0 mg) were added, and the mixture was degassed once again and then heated to 140°C for 12 h to get the polymer. The polymer solution was then precipitated into methanol and the solid was collected and dried. Then, the polymer was extracted using Soxhlet extraction from acetone, hexane and chloroform. The chloroform fraction was then concentrated and precipitated into methanol again. The deep blue solid was collected and dried to yield the polymer PBDTBT-C6C10. Yield (73 mg, 87%) ^{1}H-NMR (500MHz, $CDCl_3$, δ ppm): 9.10-7.60 (m, 2H), 4.85-3.15 (m, 6H), 2.50-0.65(m, 60H). GPC (THF), Mn=20.6 kDa, $Đ$=1.21.

M2: M2 was synthesized according to the reported procedure in reference (Nielsen et

al., 2016). ^{1}H-NMR (500MHz, $CDCl_3$, δ ppm):7.58-7.56(d, 2H),7.38-7.37(dd,2H), 4.44-4.42 (m, 4H), 3.88-3.86 (m, 4H), 3.77-3.75 (m, 4H), 3.73-3.69 (m, 4H), 3.68-3.62 (m, 4H), 3.37 (s,6H); ^{13}C-NMR (126MHz, $CDCl_3$, δppm): 144.27, 131.84, 130.29, 126.19, 120.52, 72.81, 71.92, 70.83, 70.68, 70.66, 70.62, 70.56, 70.50, 70.40, 59.01. MS (MALDI-TOF): calcd. for C28H42O10S2, 602.22, found 602.21, 625.19 (MNa^+).

M3: M2 (1.20 g, 2.0mmol) and 20 mL of dry THF was placed in a flask and cooled to-78 °C under the protection of nitrogen. Then, n-BuLi (2 mL, 5.0 mmol, 2.5 M in THF) was slowed added over 10 mins. The reaction was maintained at-78 °C for 1.5 h, then tributylchlorostannane (6 mL, 6.0 mmol, 1.0 M in THF) was added in one portion. The reaction was stirred at-78 °C for 0.5 h and allowed to slowly warm to room temperature overnight. Dichloromethane and water were added, and the organic fraction was collected and washed with water for three times. The organic fraction was concentrated and the crude M3 was purified using a silica gel column chromatography (the silica gel was soaked in trimethylamine and dried before use) with hexane:methanol (15:1 v/v) as eluent. Yield (1.36 g, 58%). ^{1}H-NMR (500MHz, $CDCl_3$, δ ppm): 7.51 (s, 2H), 4.49-4.41 (t, *J* = 5.0 Hz, 4H), 3.93-3.87 (t, *J* = 5.0 Hz, 4H), 3.77 (m, 4H), 3.71-3.61 (m, 16 H), 3.53-3.50 (m, 4H), 3.35 (s, 6H), 1.68-1.54 (m, 12H), 1.41-1.33 (m, 12H), 1.24-1.13 (m, 12H), 0.90 (t, *J* = 7.3 Hz, 18H). ^{13}C NMR (126 MHz, $CDCl_3$, δ ppm): 142.62, 140.27, 134.28, 132.94, 128.12, 72.48, 71.93, 70.84, 70.73, 70.68, 70.61, 70.55, 70.52, 59.02, 28.99, 27.26, 13.70, 10.86. MS (MALDI-TOF): calcd. for C52H94O10S2Sn2, 1180.43 found 1203.39 (MNa^+).

M4： M4 was synthesized using the same procedure to that of M2. ^{1}H-NMR (500MHz, $CDCl_3$, δ ppm): 7.58-7.55(d,2H),7.38-7.36 (dd,2H),4.45-4.40 (m,4H),3.90-3.86 (m,4H),3.78-3.75(m,4H), 3.74-3.61 (m, 40H), 3.56-3.52 (m, 4H), 3.37 (s, 6H); ^{13}C-NMR (126MHz, $CDCl_3$, δppm): 144.27, 131.88, 130.31, 126.23, 120.52, 72.82, 71.91, 70.84, 70.67, 70.60, 70.57, 70.54, 70.48, 70.43, 59.02. MS (MALDI-TOF): calcd. for C40H66O16S2, 866.38, found 866.34.

M5: M5 was synthesized using the same procedure to that of M3. Yield(1.76 g, 61%) ^{1}H-NMR (500MHz, $CDCl_3$, δ ppm): 7.51 (s,2H),4.47-4.45(m,4H),3.91-3.89(m,4H),3.72-3.71(m,4H), 3.69-3.62(m,36H), 3.55-3.53 (m,4H), 3.37(s,6H), 1.65-1.58 (m, 12H), 1.39-1.33 (m, 12H), 1.20-1.17 (m, 12H), 0.91 (t, *J* = 7.3 Hz, 18H). MS (MALDI-TOF): calcd. for C64H118O16S2Sn2, 1444.59, found 1444.54, 1467.53 (MNa^+).

PBDTBT-4EO: M3 (118.1 mg, 0.1 mmol) and 5,6-difluoro-4,7-diiodobenzo[c][1,2,5]thiadiazole (42.4 mg, 0.1 mmol) were placed were placed in a round-bottomed flask, then CB (0.5 mL) and DMF (0.5 mL) were added. The mixture was then degassed for three times to remove the oxygen. Then $Pd_2(dba)_3$ (1.0 mg) and $P(o\text{-}tol)_3$ (2.0 mg) were added, and the mixture was degassed once again and then heated to 140°C for 12 h to get the polymer. The polymer solution was then precipitated into acetone and the solid was collected and dried. Then, the polymer was extracted using Soxhlet extraction from acetone, hexane, and chloroform. The chloroform fraction was then concentrated and precipitated into acetone again. The deep blue solid

was collected and dried to yield the polymer PBDTBT-4EO. Yield (70 mg, 91%) ^{1}H-NMR (500MHz, $CDCl_3$, δ ppm): 8.70-7.60 (m, 2H), 4.90-3.10 (m, 38H). GPC (THF), Mn=26.5kDa, *Đ*=1.57.

PBDTBT-7EO: PBDTBT-7EO was synthesized using the same procedure with that of PBDTBT-4EO. Yield (89 mg, 86%) ^{1}H-NMR (500MHz, $CDCl_3$, δ ppm): 8.75-7.80 (m, 2H),4.85-3.25 (m,38H). GPC (THF), Mn=29.6kDa, Đ=3.85.

Characterization: ^{1}H NMR and ^{13}C NMR spectra of the monomers and polymers were recorded on a Bruker AV-600 spectrometer with $CDCl_3$ as solvent. Molecular weights of polymers were determined by a Waters GPC 2410 with a refractive index (RI) detector and using a calibration curve with polystyrene standards where THF was used as mobile phase. UV-vis spectra of the polymers were collected on a HP 8453 spectrophotometer. For the solution absorption, the polymers were dissolved into $CHCl_3$ with a concentration of 0.02 mg mL^{-1}. Samples for film absorption of these polymers were prepared by spin-coating their solutions (10 mg mL^{-1}) into quartz glasses. Photoluminescence (PL) spectra were measured using a Jobin-Yvon spectrofluorometer. Cyclic Voltammetry (CV) measurements were conducted in a CHI660E elctrochemical work-stastation where a glassy carbon electrode was used as working electrode. An Ag/AgCl electrode was used as reference electrode and a Pt wire was used as counter electrode. The measurements were conducted in anhydrous acetontrile with tetrabutylammonium hexafluorophosphate (Bu_4NPF_6, 0.1 M) as supporting electrolyte under argon atmosphere. The scan rate is 0.05 V/s. The potential of the Ag/AgCl electrode was calibrated using the ferrocene/ferrocenium (Fc/Fc^{+}), which delivered a reduction potential of -4.8 eV. X-ray photoelectronic spectroscopy (XPS) was measured on a Thermo Electron ESCALAB 250 spectrometer equipped with a monochromatic Al X-ray source (1486.6 eV). Water contact angle measurements were performed on a VCA15 surface contact angle analyzer (Dataphysics). UPS measurements were performed on the Thermo ESCALAB 250XI. The Valance band (*VB)* spectra were measured with a monochromatic He I light source (21.2 eV) and a VG Scienta R4000 analyzer. A sample bias of-5 V was applied to observe the secondary electron cutoff. The FT-IR spectra of these polymers were obtained from VERTEX 70(Bruker). X-ray powder diffraction of these polymers in powder state was performed on Bruker D8 ADVANCE. The high resolution transmission electron microscope (HR-TEM) images of the dispersed polmers was obtained from TF20, Joel 2100F Microscope.

Electrochemical Analysis. The electrochemical experiments were conducted with a CHI660E Electrochemical System in a three electrode cell with a Pt sheet as the counter electrode and an Ag/AgCl electrode (3 M KCl) as the reference electrode. The working electrodes were prepared by coating polymers (10 mg mL^{-1} in $CHCl_3$) onto ITO glasses with thicknesses about 300 nm. The active area is confined to 0.50 cm^2. A 0.1 M Na_2SO_4 aqueous solution (pH = 6.8) was chosen as the supporting electrolyte and was purged with nitrogen for 30 min to remove O_2 before any measurements. The working electrodes for photocurrent test were illuminated with a solar simulator (300-W Xe light source, λ > 300 nm). For Mott-Schottky plots, the E_{FB} was extracted from Mott-Schottky

equation: $\frac{1}{C^2} = \frac{2(E-E_{FB}-k_B\mathrm{T/e})}{\varepsilon\varepsilon_0 \mathrm{A}^2 e N_D}$. According to this Equation, a straight tangent line can be drawn by using a plot of $1/C^2$ vs E, and E_{FB} can be determined by the intercept of the straight line with E axis.

Photocatalytic hydrogen evolution: The hydrogen evolution measurements were performed on a Labsolar-IIIAG photocatalytic system (PerfectLight) equipped with a 50-mL reactor. For the photocatalytic experiment, polymers (2.5 mg) were firstly dissolved in 250 μL of THF and then dispersed into a mixture of 50 mL of AA solution (0.2 M, pH = 4.0 adjusted by NaOH aq.). The total concentration of the polymers for photocatalytic measurement in reaction solution was 50 μg/mL. The reaction was held in a vacuum for 30 min to remove the dissolved oxygen and THF, followed by ultrasonication for 1 h. The photocatalytic experiments were then degassed again and illuminated with a solar simulator (300-W Xe light source, λ > 300 nm). Pt co-catalysts were prepared by dissolving H_2PtCl_4 into the polymer solution with irradiation for 1 h, which enables the formation of Pt nanoparticles (Chen et al., 2017). The calculated weight of Pt co-catalysts is 3% of that of each polymer. The luminous power reaching the surface of the reaction solution was calibrated to be 162.4 mW cm^{-2} by a power meter. The produced gas was analysed by a GC7900 gas chromatograph. Hydrogen was detected with a thermal conductivity detector, referencing against standard gas with a known concentration of hydrogen. The AQY was measured at selected wavelengths enabled by different band pass filters (CELQD, 380, 420, 450, 550, 600, 650 and 700 nm). The AQY at a given wavelength was calculated from the following equations:

$N_o=(E\lambda T\%)/hc$; $N=(V\times 6.02\times 10^{23})/(22.4t)$;$AQY=2N/No$

N_o represents the number of incident photons, N represents the number of collected H_2 molecules, E represents the energy of incident light at a given wavelength, determined by a calibrated power meter, λ represents the wavelength of incident light, V represents the volume of H_2 molecules detected in a fixed time (t), determined by GC, T% represents the transmittance of the quartz cell.

References:

Maruyama, T., and Yamamoto, T. (1997). Effective photocatalytic system based on chelating π-conjugated poly(2,2′-bipyridine-5,5′-diyl) and platinum for photoevolution of H_2 from aqueous media and spectroscopic analysis of the catalyst. *J. Phys. Chem. B* 101, 3806.

Yang, C., Ma, B. C., Zhang, L., Lin, S., Ghasimi, S., Landfester, K., Zhang, K. A. I., and Wang, X. (2016) Molecular engineering of conjugated polybenzothiadiazoles for enhanced hydrogen production by photosynthesis. *Angew. Chem. Int. Ed*. 55, 9202.

Sprick, R. S., Bonillo, B., Clowes, R., Guiglion, P., Brownbill, N. J., Slater, B. J., Blanc, F., Zwijnenburg, M. A., Adams, D. J., and Cooper, A. I. (2016). Visible-light-driven hydrogen evolution using planarized conjugated polymer photocatalysts. *Angew. Chem. Int. Ed*. 55, 1792.

Li, L., Hadt, R. G.,Yao, S., Lo, W.-Y., Cai, Z., Wu, Q., Pandit, B., Chen, L.-X., and Yu, L. (2016). Photocatalysts based on cobalt-chelating conjugated polymers for hydrogen evolution from water. *Chem. Mater.* 28, 5394.

Lu, H., Hu, R., Bai, H., Chen, H., Lv, F., Liu, L., Wang, S., and Tian, H. (2017). Efficient Conjugated polymer–methyl viologen electron transfer system for controlled photo-driven hydrogen evolution. *ACS Appl. Mater. Interfaces 9*, 10355.

Zong, X., Miao, X., Hua, S., An, L., Gao, X., Jiang, W., Qu, D., Zhou, Z., Liu, X.and Sun, L. (2017). Structure defects assisted photocatalytic H_2 production for polythiophene nanofibers. *Appl. Catal. B-Environ.* 211, 98.

Wang, L., Fernández-Terán, R., Zhang, L., Fernandes, D. L., Tian, L., Chen, H., and Tian, H. (2016). Organic polymer dots as photocatalysts for visible light-driven hydrogen generation. *Angew. Chem. Int. Ed*. 55, 12306.

Pati, P. B., Damas, G., Tian, L., Fernandes, D. L. A., Zhang, L., Pehlivan, I. B., Edvinsson, T., Araujo, C. M., and Tian, H. (2017). An experimental and theoretical study of an efficient polymer nano-photocatalyst for hydrogen evolution. *Energy Environ. Sci*. 10, 1372.

Woods, D. J., Sprick, R. S., Smith, C. L., Cowan, A. J., and Cooper, A. I. (2017). A solution-processable polymer photocatalyst for hydrogen evolution from water. *Adv. Energy Mater.* 7, 1700479.

Tseng, P.-J., Chang, C.-L., Chan, Y.-H., Ting, L.-Y., Chen, P.-Y., Liao, C.-H., Tsai, M.-Li and Chou, H.-H. (2018) Design and synthesis of cycloplatinated polymer dots as photocatalysts for visible-light-driven hydrogen evolution. *ACS Catal*. 8, 7766.

Wang, X., Maeda, K., Thomas, A., Takanabe, K., Xin, G., Carlsson, J. M., Domen, K., and Antonietti, M. (2009). A metal-free polymeric photocatalyst for hydrogen production from water under visible light. *Nat. Mater.* 8, 76.

Schwinghammer, K., Tuffy, B., Mesch, M. B., Wirnhier, E., Martineau, C., Taulelle, F., Schnick, W., Senker, J., and Lotsch, B. V. (2013). Triazine-based carbon nitrides for visible-light-driven hydrogen evolution. *Angew. Chem. Int. Ed*. 52, 2435.

Lin, L., Ou, H., Zhang, Y., and Wang, X. (2016). Tri-s-triazine-based crystalline graphitic carbon nitrides for highly efficient hydrogen evolution photocatalysis. *ACS Catal*. 6, 3921.

Martin, D. J., Qiu, K., Shevlin, S. A., Handoko, A. D., Chen, X., Guo, Z., and Tang, J. (2014). Highly efficient photocatalytic H_2 evolution from water using visible light and structure-controlled graphitic carbon nitride. *Angew. Chem. Int. Ed.* 53, 9240.

Yu, Y., Yan, W., Wang, X., Li, P., Gao, W., Zou, H., Wu, S., and Ding, K. (2018). Surface engineering for extremely enhanced charge separation and photocatalytic hydrogen evolution on g-C_3N_4. *Adv. Mater.* 30, 1705060.

Schwab, M. G., Hamburger, M., Feng, X., Shu, J., Spiess, H. W., Wang, X., Antonietti, M., and Müllen,

K. (2010). Photocatalytic hydrogen evolution through fully conjugated poly(azomethine). networks. *Chem. Commun*. 46, 8932.

Sprick, R. S., Jiang, J. –X.,Bonillo, B., Ren, S., Ratvijitvech,T., Guiglion,P., Zwijnenburg, M. A., Adams, D. J., and Cooper, A. I. (2015). Tunable organic photocatalysts for visible-light-driven hydrogen evolution. *J. Am. Chem. Soc.* 137, 3265.

Stegbauer, L., Schwinghammer, K., and Lotsch, B. V. (2014). A hydrazone-based covalent organic framework for photocatalytic hydrogen production. *Chem. Sci.* 5, 2789.

Vyas, V., Haase, F., Stegbauer, L., Savasci, G., Podjaski, F., Ochsenfeld, C., and Lotsch, B. V. (2015). A tunable azine covalent organic framework platform for visible light-induced hydrogen generation. *Nat. Commun*. 6, 8508.

Park, J. H., Ko, K. C., Park, N., Shin, H.–W., Kim, E., Kang, N., Ko, J. H., Lee, S. M., Kim, H. J., Ahn, T. K., Lee, J. Y., and Son, S. U. (2014). Microporous organic nanorods with electronic push–pull skeletons for visible light-induced hydrogen evolution from water. *J. Mater. Chem. A* 2, 7656.

Schwinghammer, K., Hug, S., Mesch, M. B., Senker, J., and Lotsch, B. V. (2015). Phenyl-triazine oligomers for light-driven hydrogen evolution. *Energy Environ. Sci*. 8, 3345.

Yang, C., Ma, B. C., Zhang, L., Lin, S., Ghasimi, S., Landfester, K., Zhang, K. A. I., and Wang, X. (2016). Molecular engineering of conjugated polybenzothiadiazoles for enhanced hydrogen production by photosynthesis. *Angew. Chem. Int. Ed*. 128, 9202.

Li, L., Cai, Z., Wu, Q., Lo, W-Y., Zhang, N., Chen, L. X., and Yu, L. (2016). Rational design of porous conjugated polymers and roles of residual palladium for photocatalytic hydrogen production. *J. Am. Chem. Soc*. 138, 7681.

Wang, N., Chen, Z., Wei, W., and Jiang, Z. (2013). Fluorinated benzothiadiazole-based conjugated polymers for high-performance polymer solar cells without any processing additives or post-treatments. *J. Am. Chem. Soc*. 135, 17060

Nielsen, C. B., Giovannitti, A., Sbircea, D.T., Bandiello, E., Niazi, M. R., Hanifi, D. A., Sessolo, M., Amassian, A., Malliaras, G., Rivnay, J., and McCulloch. I. (2016). Molecular design of semiconducting polymers for high-performance organic electrochemical transistors. *J. Am. Chem. Soc.* 138, 10252.

Chen, J., Dong, C.-L., Zhao, D., Huang, Y.-C., Wang, X., Samad, L., Dang, L., Shearer, M., Shen, S., and Guo, L. (2017). Molecular design of polymer heterojunctions for efficient solar–hydrogen conversion. *Adv. Mater.* 29, 1606198.

Shibata, T., Kabumoto, A., Shiragami, T., Ishitani, O., Pac, C., and Yanagida, S. (1990). Novel visible-light-driven photocatalyst. poly(p-phenylene)-catalyzed photoreductions of water, carbonyl compounds, and olefins. *J. Phys. Chem*. 94, 2068.